

Imaging in optical micromanipulation using two-photon excitation

This article has been downloaded from IOPscience. Please scroll down to see the full text article.

2004 New J. Phys. 6 136

(<http://iopscience.iop.org/1367-2630/6/1/136>)

View [the table of contents for this issue](#), or go to the [journal homepage](#) for more

Download details:

IP Address: 38.107.179.214

The article was downloaded on 20/02/2012 at 22:11

Please note that [terms and conditions apply](#).

Imaging in optical micromanipulation using two-photon excitation

K Dholakia, H Little, C T A Brown, B Agate, D McGloin, L Paterson and W Sibbett

School of Physics and Astronomy, University of St Andrews, North Haugh, Fife, KY16 9SS, UK

E-mail: kd1@st-and.ac.uk

New Journal of Physics **6** (2004) 136

Received 28 July 2004

Published 21 October 2004

Online at <http://www.njp.org/>

doi:10.1088/1367-2630/6/1/136

Abstract. Recent studies have realized optical micromanipulation of extended two- and three-dimensional structures and optical binding. In many recent experiments the optical interaction between particles and their light scattering has played a key role. We use fluorescein dye within the sample medium and a femtosecond laser for optical micromanipulation. By the process of two-photon excitation we can directly observe how the light behaves during refraction and reflection within a sample of optically guided microspheres. We directly visualize the reconstruction of the Bessel light beam by excitation of two-photon fluorescence when used as an optical guide for microscopic particles dispersed within this dyed medium. This technique may assist in the visualization of optical scattering and refraction in micromanipulation and the creation of large optically bound matter crystals.

Contents

1. Introduction	2
2. Experiment	2
3. Results	5
Acknowledgments	7
References	7

1. Introduction

The mechanical forces of light on microscopic particles are limited to forces in the pico-Newton range. However, these forces are sufficient to trap and guide microparticles. The optical gradient force can trap objects at the most intense part of a focused light beam and this is known commonly as optical tweezers [1]. In optical guiding the gradient force works in two dimensions to pull the particle towards the beam propagation axis and the scattering force propels the particle along the beam axis [2]. Such optical micromanipulation has seen significant expansion in recent years and a variety of important experiments have been performed. Advanced light pattern configurations have resulted in two- and three-dimensional structures [3] that have applications in colloid science and biology. Importantly the scattering and refraction of light by each of the trapped objects in extended light patterns plays a central role in extended trapped structures. Optical binding is an example where trapped objects take up key positions in the light field directly related to the exact nature of the scattering and refraction of light [4]–[6]. The creation of very large extended structures also may depend critically upon how each localized object effects the incident light field. Another example is the use of the self-healing Bessel light beam [7] where the light beam reforms around obstacles allowing for the alignment of multiple objects separated by millimetre distances [8].

In this paper we demonstrate a novel optical imaging method for micromanipulation that allows us to observe the optical light fields within a medium after they undergo refraction and scattering from microparticles. The technique is based around the use of fluorescein dye in the sample medium. By using a femtosecond laser for optical micromanipulation we can use the fact that the peak power of the beam can readily initiate two-photon excitation. As two-photon excitation requires a high intensity of light, and is readily diminished by scattering, it can offer an *in situ* signature of the optical beam intensity in micromanipulation experiments. Two-photon excitation has a small cross section and thus can only occur at points of sufficient photon flux. The light emission in this process is thus highly discriminate and has a low background as the emitted light is not at the fundamental wavelength. We demonstrate the versatility of this imaging technique by showing for the first time the optical beam path in Bessel beam reconstruction as the beam undergoes scattering from a guided microsphere.

2. Experiment

The experimental setup has been described previously [9] and is illustrated in figure 1(a). An axicon generated Bessel beam is generated using a Ti-sapphire femtosecond laser. The Bessel beam produced by the axicon is illustrated in the inset of figure 1(b). The central maximum diameter was measured to be $30\ \mu\text{m}$. In order to produce the $3\text{--}4\ \mu\text{m}$ central maximum diameter required for our experiments, the Bessel beam is passed through a $\times 10$ demagnifying telescope. The resulting beam has a ‘diffraction-free’ propagation distance of approximately 3 mm. The beam is directed horizontally through a glass cuvette ($2\ \text{mm} \times 2\ \text{mm} \times 20\ \text{mm}$) which contains silica microspheres ranging in size from 5 to $10\ \mu\text{m}$ dispersed in water containing a saturated solution of fluorescein dye. Observation was orthogonal to the beam-propagation direction, using a CCD camera, microscope objective and monitor.

The zeroth-order Bessel light beam is a solution of the vector Helmholtz equation, approximately described by the scalar Helmholtz equation. It is propagation invariant because

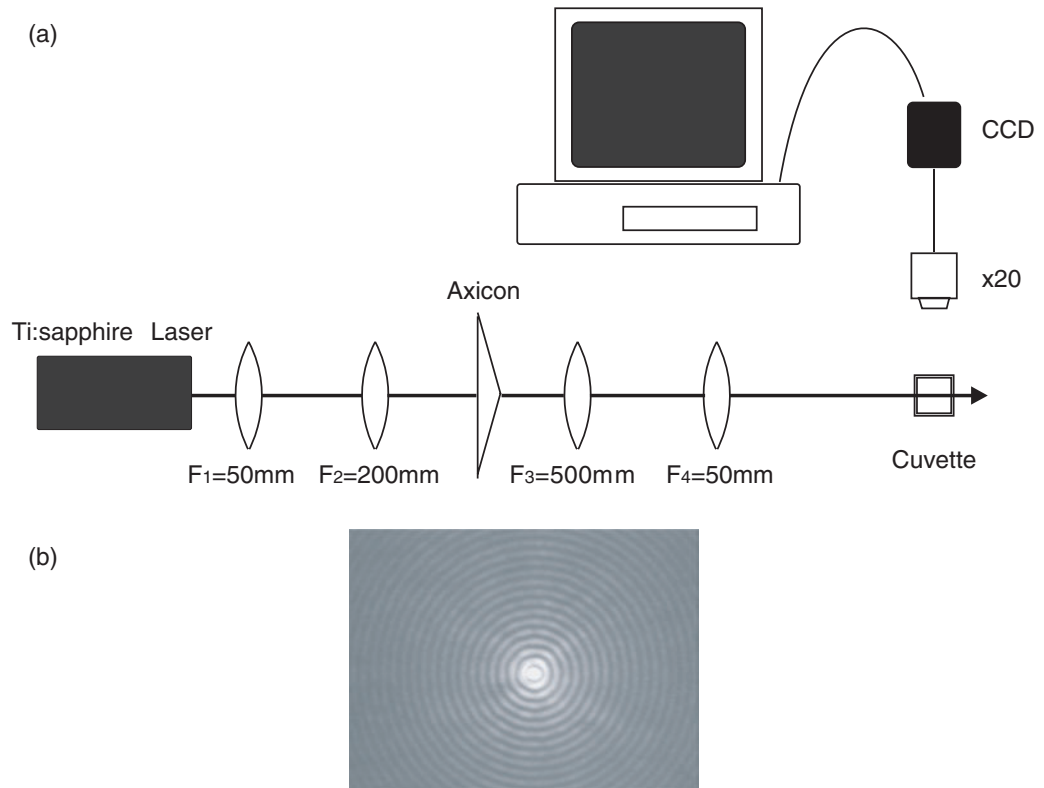


Figure 1. (a) Experimental arrangement for the generation of the femtosecond Bessel beam and subsequent guiding experiments. The view is from above. (b) The profile of a typical Bessel beam generated by the axicon element.

the transverse profile of the beam remains unaltered during free-space propagation and may be deemed ‘non-diffracting’. The electric field amplitude of a zeroth-order Bessel beam is given by

$$E(r, z) = A \exp(ik_z z) J_0(k_r r). \quad (1)$$

Here J_0 is the zeroth-order Bessel function and k_r and k_z are the radial and longitudinal components of the free-space wavevector k where $k = 2\pi/\lambda$. An ideal zeroth-order Bessel beam would consist of an infinite number of rings around a central maximum. However, such a beam would require infinite energy. A finite approximation to a Bessel beam is realized efficiently using a conical glass element known as an axicon. The light is refracted in such an element and the emergent beam has wavevectors lying on a conical surface. Such a distribution of wavevectors is a central characteristic of a Bessel light beam. The axicon generated beam is a close approximation to a Bessel light beam over a given distance. For an axicon of opening angle γ , refractive index n , illuminated with a Gaussian light beam of beam waist w_0 the propagation distance is given by

$$Z_{\max} \approx \frac{w_0}{(n-1)\gamma}. \quad (2)$$

The central maximum propagates for several Rayleigh ranges without appreciable spreading and thus offers a focal line of light which has been used for extended guiding of microscopic objects [10].

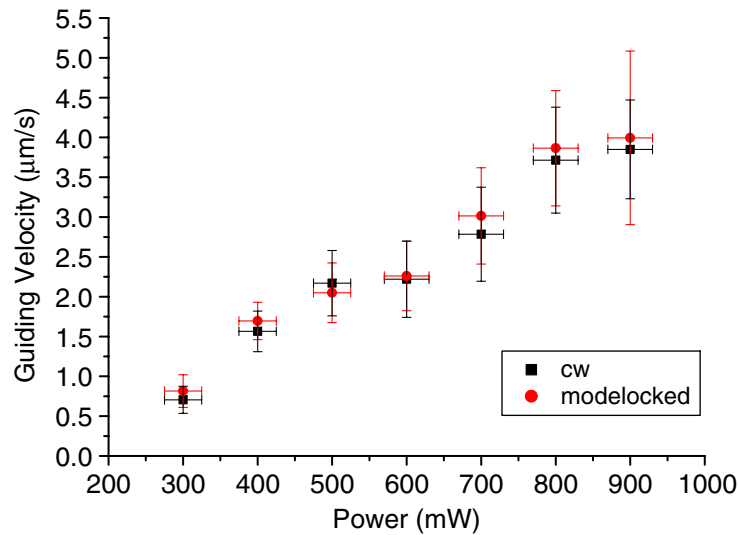


Figure 2. A comparison of the guiding velocities obtained for $1\ \mu\text{m}$ diameter silica spheres for CW (black squares) and femtosecond pulses (red circles) for a range of incident laser powers.

The outer rings of the Bessel beam act to replenish the central maximum and prohibit it from spreading. Such self-healing or self-reconstruction of the light field has been observed in previous studies and used for simultaneous micromanipulation in multiple planes. However, whilst a cross section of the light field at various points along its propagation distance may be recorded, a direct visualization of the conical wave-vectors, the diffraction and subsequent reformation of the beam around a microsphere acting as an obstacle has not been observed. Here we present the first direct visualization of this process by two-photon excitation within the sample medium elucidating the intensity profile of the beam at various stages in its propagation.

The Ti:sapphire laser can be operated in two regimes, continuous wave (CW) and mode-locked. The mode-locked output has a pulse duration, measured by autocorrelation, of 100 fs at a pulse repetition frequency of 80 MHz and up to 900 mW output power. This corresponds to a pulse energy of $11\ \text{nJ pulse}^{-1}$ and the pulses have a peak power of approximately 110 kW. The fluorescein dye has a broad absorption band centred around 480 nm with an emission band centred around 530 nm. When the mode-locked emission from the laser described above passes through the cuvette containing the fluorescein dye, a streak of fluorescence corresponding to the laser beam is observed. When the laser operates in the CW regime, no fluorescence is observed. We interpret this behaviour as evidence of a two-photon absorption process in the dye that leads to the fluorescence observed when using the mode-locked laser. Previous experiments, with no dye present in the cuvette, demonstrated the ability of this beam to trap and guide particles in the same way as expected for a corresponding CW beam [9]. Figure 2 illustrates a comparison of guiding velocities obtained for $1\ \mu\text{m}$ spheres using CW and mode-locked beams with the same incident power showing that it is the average power that dominates optical guiding.

3. Results

In figure 3(a) we observe the two-photon signal from the fluorescein dye excited by the Bessel beam in the sample chamber as the beam encounters and guides a $5\ \mu\text{m}$ sphere. The power in the Bessel beam at the cuvette is 750 mW, corresponding to a power in the central maximum of 25 mW. The beam distortion along the axis is delineated by the absence of a two-photon signal immediately in front of the guided sphere and conical refraction of rays may be observed in the vicinity of the sphere. Approximately $90\ \mu\text{m}$ in front of the sphere we can observe self-healing of the beam: the signature of this is the reformation of the central maximum of the beam immediately prior to encountering the next guided particle. This also verifies an important aspect of Bessel-beam guiding previously not seen: reconstruction of the beam plays a key role in creating extended conveyor belts of guided microparticles. In figure 3(b), we observe the guiding of multiple particles in the Bessel beam with the same incident power. The first particle is trapped and the Bessel beam diffracts and is reformed in a similar process to that illustrated in figure 3(a). Further along the beam, a second particle is trapped and again the Bessel beam is diffracted and reformed. In practice, we have used these beams to trap and guide many particles across the whole width of the cuvette. Furthermore, we have also demonstrated, in a previous work [9] that the combination of the Bessel beam with the short pulses from the fs-laser can allow non-linear optical processes to take place throughout the whole array of guided particles. For comparison, in figure 3(c), we illustrate the behaviour of a Gaussian beam with a focused spot size and an incident power of 750 mW corresponding to the central maximum diameter of our Bessel beam. In this case, a bright streak of two-photon-induced fluorescence is observed in the peak of the focussing beam. When the Gaussian beam strikes a sphere, scattering occurs and no beam reformation can be observed. The residual fluorescence is from the fraction of the beam that passes through the transparent sphere. When using the Gaussian beam, it is not possible to replicate the guiding behaviour observed with the Bessel beam. This confirms previous studies that show Bessel guiding offering significant advantages over longer distances [10].

In figure 4 we show a numerical simulation using a beam propagation algorithm of a Bessel beam as it encounters a thin opaque obstacle. We do not take into account any scattering or refraction the light experiences on encountering the particle. We model the observed Bessel beam within the cuvette rather than model the propagation of the beam through the experimental axicon and telescope. Thus the axicon opening angle in the model is approximately 18° creating a beam with a central core of $\sim 4\ \mu\text{m}$. To produce the correct propagation distance ($\sim 3\ \text{mm}$) a beam waist of 0.46 mm is used. This produces a Bessel beam which accurately describes the experimentally observed beam. The model has a good agreement with the observed reconstruction distances, although it requires that a slightly larger particle ($8\ \mu\text{m}$) is used. We can see the light diffracted around the object and also the reconstruction of the beam. The qualitative agreement between figures 3(a) and 4 show the potential of this imaging technique, allowing us to visualize the intensity of the propagating beam, and we believe that significant further optimization will allow direct observation of a range of interference-based optical phenomena in detail. The major difference between the model and the experimental images is that the model displays the whole Bessel beam, in the experimental situation only the central core, where the intensity is high enough to excite a two-photon emission, is seen.

In optical binding the very scattering and refraction from microspheres creates *in situ* equilibrium positions within which other spheres may reside [4]. Recent simulations have shown how light fields behave in the vicinity of these spheres [5]. Such optical binding offers new

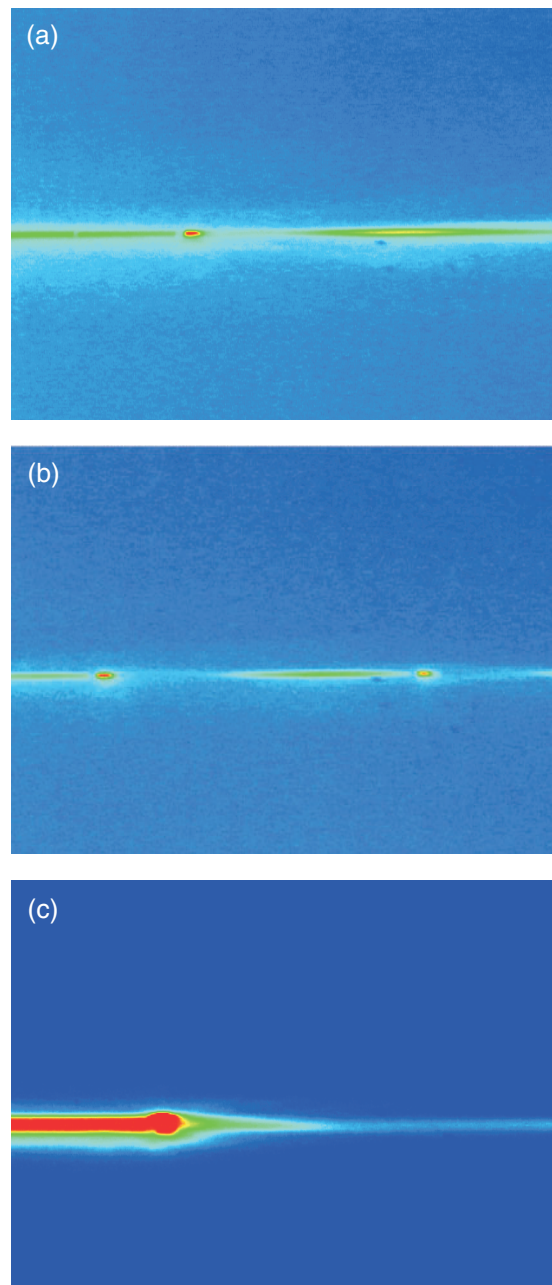


Figure 3. Two-photon absorption-induced fluorescence obtained when trapping and guiding $5\ \mu\text{m}$ spheres with 750 mW power from the mode-locked laser incident on the cuvette. (a) Bessel beam incident with $3\text{--}4\ \mu\text{m}$ central maximum diameter. The beam is scattered by the sphere before reforming approximately $90\ \mu\text{m}$ in front of the trapped sphere. (b) Bessel beam incident with $3\text{--}4\ \mu\text{m}$ central maximum diameter. A second sphere is now also trapped in front of the first sphere. Again, the start of the process of beam reformation can be seen to the right of the second trapped sphere (see also the [movie](#)). (c) The trapping of a single sphere by a Gaussian beam with a $4\ \mu\text{m}$ diameter beam. No beam reformation is detected in this case as observed by the absence of two-photon excitation beyond the sphere position.

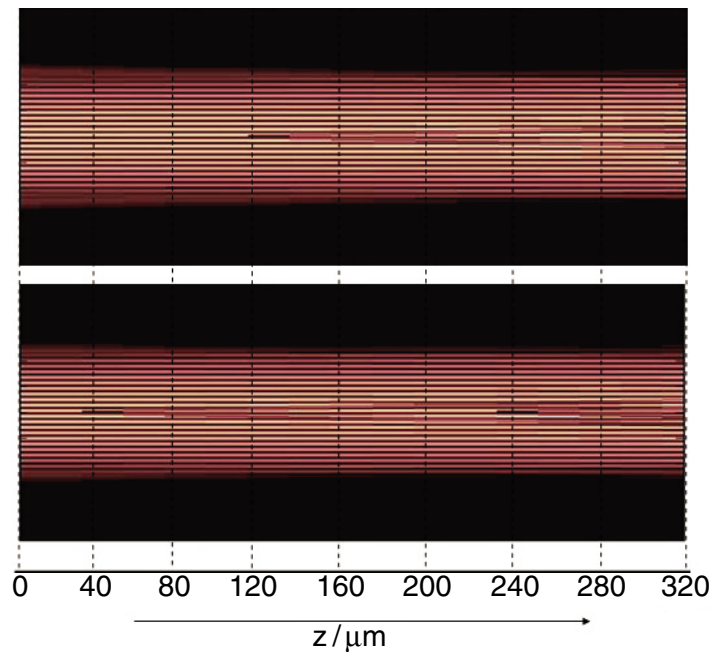


Figure 4. Numerical simulation of a Bessel beam with a $4\ \mu\text{m}$ central maximum diameter striking a $4\ \mu\text{m}$ diameter obstacle. The view is from the side, along the beam propagation length. Again, reformation of the beam can be seen approximately $90\ \mu\text{m}$ in front of the scattering object, in qualitative agreement with our experimental results.

mechanisms by which we can create large-scale arrays of microparticles and shows extended systems that even have analogues to atomic systems.

The use of dynamic light patterns in 3D in optical micromanipulation is also an emergent area where our imaging technique may find application. Spatial light modulators can arrange some tens of particles into crystal arrays [11, 12] and an exact understanding of the light particle interaction using our methodology can help elucidate the exact light pattern required in a given plane taking into account even distortions induced in previous two-dimensional planes of the optical pattern.

Acknowledgments

We thank the Scottish Higher Education Funding Council, the Royal Society and EPSRC for support.

References

- [1] Ashkin A, Dziedzic J M, Bjorkholm J E and Chu S 1986 *Opt. Lett.* **11** 288
- [2] Ashkin A 1971 *Appl. Phys. Lett.* **19** 283
- [3] MacDonald M P, Paterson L, Volke-Sepulveda K, Arlt J, Sibbett W and Dholakia K 2002 *Science* **296** 1101
- [4] Tatarikova S A, Carruthers A and Dholakia K 2002 *Phys. Rev. Lett.* **89** 283901
- [5] McGloin D, Carruthers A, Dholakia K and Wright E 2004 *Phys. Rev. E* **69** 024103
- [6] Burns M M, Fournier J and Golovchenko J 1990 *Science* **249** 749

- [7] Durnin J 1987 *J. Opt. Soc. Am. A* **4** 651
- [8] Garcés-Chávez V, McGloin D, Melville H, Sibbett W and Dholakia K 2002 *Nature* **419** 145
- [9] Little H, Brown C T A, Garcés-Chávez V, Sibbett W and Dholakia K 2004 *Opt. Express* **12** 2560
- [10] Tatarkova S A, Sibbett W and Dholakia K 2003 *Phys. Rev. Lett.* **91** 038101
- [11] Melville H, Milne G F, Spalding G C, Sibbett W, Dholakia K and McGloin D 2003 *Opt. Express* **11** 3562
- [12] Leach J, Sinclair G, Jordan P, Courtial J and Padgett M J 2004 *Opt. Express* **12** 220